

Competition between strain and chemistry effects on adhesion of Si and SiC

Y. Liu and I. Szlufarska

Materials Science and Engineering, University of Wisconsin–Madison, Madison, Wisconsin 53706, USA

(Received 2 February 2009; published 23 March 2009)

We use *ab initio* calculations to demonstrate that adhesion of Si and SiC depends on the interplay between surface strain and chemistry. We discover that work of adhesion of Si depends linearly on surface strain. Compressive surface strain increases adhesion, which explains why bare Si-terminated SiC has larger adhesion than Si. However, with as little as one monolayer of oxygen coverage, adhesion of SiC becomes negligible while adhesion of Si remains finite irrespectively of the specific oxygen configuration. This effect is due to fundamental differences between reactivities of Si and SiC during the early stages of oxidation.

DOI: [10.1103/PhysRevB.79.094109](https://doi.org/10.1103/PhysRevB.79.094109)

PACS number(s): 81.65.Rv, 68.35.Np, 68.35.Gy

I. INTRODUCTION

Understanding adhesion from atomistic and molecular perspective is essential for design of reliable devices with dimensions in the nanometer regime. Because of the large surface-to-volume ratio, surface forces play a key role in any nanoscale design where two materials are in contact. Undesired adhesion has been shown to be prohibitive for successful operation of microelectromechanical and nanoelectromechanical systems (MEMS/NEMS).^{1–3} MEMS and NEMS devices are typically built of silicon because of its well developed fabrication capabilities. One way to reduce the large adhesion of Si is by coating the surfaces with a thin layer of another material. Silicon carbide is particularly promising in this regard⁴ because of its outstanding mechanical properties, e.g., high hardness, high Young's modulus, and excellent wear resistance. In comparison to Si, SiC exhibits also superior oxidation resistance and better structural stability at high temperatures, which opens up the possibility of designing MEMS/NEMS devices for operations in harsh environments.⁵

Work of adhesion W_{adh} is defined as the change in surface energy per unit area when bringing two surfaces together from infinity to the equilibrium interfacial separation. W_{adh} is often determined in scanning force microscopy (SFM) experiments^{6–8} by measuring a pull-off force between the SFM tip and a sample or in beam detachment experiments by measuring stiction of a cantilever beam to a surface.⁹ A particular challenge in understanding fundamental mechanisms of adhesion is that one cannot easily correlate measured forces and energies with chemistry of the surfaces in contact. SFM experiments in which surface characterization is carried out *in situ* are still not common for tribological studies.

There have been a limited number of experiments addressing the issue of adhesion of SiC. An example of such study has been reported by Gao *et al.*,¹⁰ who investigated adhesion properties of polycrystalline cubic SiC and polycrystalline Si. It was shown that adhesion of SiC is almost 4 orders of magnitude lower than adhesion of Si. Differences in surface topographies and in oxidation rates between Si and SiC were suggested to be responsible for the lower adhesion of SiC. Additional factors that can lead to differences between adhesion of Si and SiC are polarization of Si-C bonds and surface strain that is present on Si- and C-terminated SiC

due to lattice mismatch between Si, SiC, and C. Humidity and capillary forces will also contribute to adhesion when it is measured in ambient conditions such as those reported in Ref. 10. In order to isolate the different contributions to adhesion it is necessary to carry out focused studies on well defined interfaces. In particular, the effects of surface strain and surface chemistry can be estimated with high accuracy by means of *ab initio* calculations, in which energies and structures are determined directly from quantum-mechanical principles. For example, *ab initio* calculations based on the density-functional theory (DFT) have been previously employed by Qi and Hector¹¹ to determine the type of chemical bonding that underlies adhesion between diamond and Al surfaces.

Previous *ab initio* simulations of SiC surfaces have been focused primarily on determination of the most stable surface reconstructions¹² and their chemical reactivities.^{13,14} For adhesion studies, only interfaces with other materials, e.g., AlN (Ref. 15) and BP (Ref. 15) and Ti,¹⁶ have been considered. Here we carry out DFT-based calculations in order to determine the role that surface strain and surface chemistry play in adhesion of Si and SiC during the early stages of oxidation. In order to separate the effects of strain and chemistry, we systematically consider first bare surfaces and then surfaces with increasing oxygen coverage. Such fundamental study is a necessary first step toward understanding of the mechanisms underlying reduced adhesion of SiC in conditions encountered in MEMS/NEMS applications. In our studies both Si and SiC have zinc-blende structures and are terminated with a Si layer in the (2×1) reconstruction. Both materials have many possible surface reconstructions that are close in energy and the (2×1) reconstruction is one of the most stable ones. Our simulations show that there is a large difference in adhesion trends of the two materials.

II. COMPUTATIONAL APPROACH

We employ DFT as implemented in the Vienna *Ab Initio* Simulation Package (VASP).^{17,18} General gradient approximation (GGA) is selected for evaluating electron exchange and correlation functionals. Projector augmented wave (PAW) method with 520 eV energy cutoff is used to ensure high accuracy. Wave function is expanded at Γ point in the Brillouin zone during the relaxation. Atoms are fully relaxed

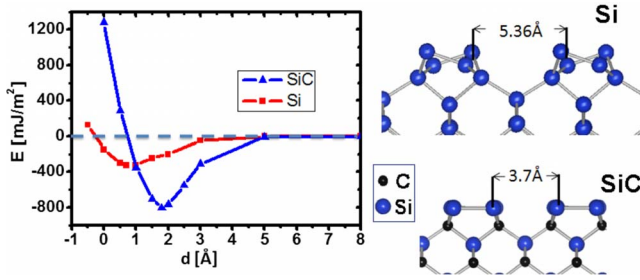


FIG. 1. (Color online) Left: energy-distance curves for bare Si (squares) and SiC (triangles). Dashed line is added to represent the reference energy state corresponding to large interfacial separation. Right: Si and SiC (001) surfaces in the (2×1) reconstructions. Dimer length and interdimer distances for Si are 2.35 and 5.37 Å, respectively. Corresponding values for SiC are 2.45 and 3.72 Å.

until all forces acting on ions are lower than $0.01 \text{ eV}/\text{Å}$ (0.016 nN).

All simulations have been performed on the (001) surfaces of Si or SiC, where SiC is terminated with a Si layer. Surfaces are simulated using 11 layer slabs with eight atoms per layer, with two identical free surfaces at both ends. The interfaces formed in such contacts are incoherent and therefore here W_{adh} is not equivalent to the cohesive energy. We report the GGA energies, however, we have also calculated energies using the local density approximation (LDA) and meta-GGA (Ref. 19) approaches. The trends reported in this paper are consistent among all three methods.

III. ADHESION OF BARE Si AND SiC

For bare Si and SiC, the total energy (E) calculated as a function of interfacial distance (d) is shown in Fig. 1. Surfaces are brought together in steps of 0.5 Å . The reference energy is taken to be that at $d=8 \text{ Å}$, i.e., when no significant interaction between surfaces can be detected. At each step the system is relaxed using the conjugate gradient method. In certain cases additional intermediate points have been calculated to ensure that the results are insensitive to the step size. For selected points *ab initio* molecular-dynamics simulations have been performed at the temperature of 300 K to search the configurational space for the global energy minimum. In this setup, W_{adh} is equal to the energy at the minimum of the E - d curve divided by the area of the interface and it is 324 mJ/m^2 (2.0 eV/nm^2) for Si and 806 mJ/m^2 (4.8 eV/nm^2) for SiC. We have investigated the same surface pairs but with one of the surfaces displaced relatively to the other within the interface plane. Since such displacement is not possible in the one-slab configuration, we carried out simulations with two small slabs. Each slab consists of five layers of atoms with the bottom two layers being fixed in space. Calculations in the two-slab configuration were performed for zero displacement and for displacements by vectors $(0.8a, 0.6a, 0)$ and $(0.3a, 0.2a, 0)$ along the (340) and (230) directions, respectively, where a is the lattice vector of the cubic unit cell. While the actual value of W_{adh} varies with the displacement, in all cases SiC exhibits larger adhesion than Si. These results suggest that bare SiC coating may

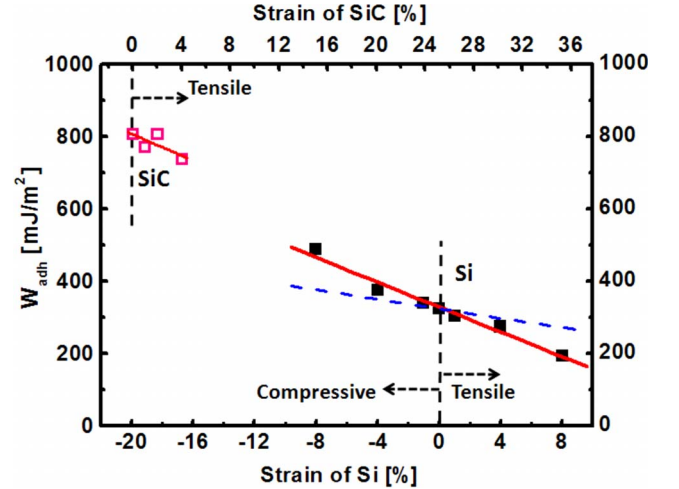


FIG. 2. (Color online) Strain effect on adhesion. Dashed vertical lines are added to mark unstrained Si and SiC. Solid and empty squares correspond to W_{adh} of Si and SiC, respectively. Solid lines represent linear fits to calculated W_{adh} as a function of strain. The slope of the fitted line for Si is $17.2 \text{ mJ/m}^2 \%$ strain. A slanted dashed line (blue) corresponds to the analytical model for W_{adh} , in which the only response to strain is a change in the contact area.

exacerbate the problem of adhesion in MEMS/NEMS rather than help reduce it.

It may seem surprising that W_{adh} of SiC is more than twice as large as that of Si. After all, both materials have the same cubic structure and similar (2×1) surface reconstruction. However, Si and SiC differ significantly in their lattice constants. The large lattice mismatch between Si and SiC introduces roughly 20% compressive strain in the Si layer that terminates SiC. Therefore in comparison to Si, SiC has smaller spacing between the (2×1) dimers as shown in Fig. 1.

In order to determine whether surface strain can account for the observed large adhesion of SiC, we calculated E - d curves for Si and SiC samples that are strained biaxially in the plane of the surface. Using the one-slab configuration we applied 1%, 2%, 4%, and 8% strains (both tensile and compressive) to Si and 1%, 2%, and 4% strains to SiC (tensile strain only). Directly applying strains on the order of 20% causes the Si and SiC surfaces to become unstable with respect to the zinc-blende structure, e.g., surfaces were observed to buckle. The dependence of the calculated W_{adh} on strain for Si and SiC is shown in Fig. 2, which reveals that tensile strain decreases adhesion and compressive strain increases it. As demonstrated in the case of Si (solid squares), the relationship between W_{adh} and strain is linear. Linear extrapolation of the Si data to large strains is largely consistent with W_{adh} of SiC (empty squares). The linear extrapolation underestimates W_{adh} of SiC by 12%. A possible reason for this difference is the fact that Si surfaces retain the initial (2×1) reconstruction as they come in contact while reconstruction of SiC changes from (2×1) to (2×2) . This additional relaxation mechanism results in a stronger interfacial bonding of SiC. Changes in surface reconstruction are not accounted for in the extrapolation of data obtained for the (2×1) reconstruction.

What is the physical origin of the linear relation between strain and W_{adh} ? We investigate whether this relation can be explained by a simple argument of scaling of the contact area. Namely, W_{adh} can be estimated as the number of bonds formed across the interface (N) multiplied by an average energy (E_b) per interfacial bond and divided by the surface area (A), i.e., $W_{\text{adh}} = NE_b/A$. We first assume that both N and E_b are constant during deformation and only A changes in response to strain. If strain ϵ is applied in plane of the surface so that $A = A_0(1 + \epsilon)^2$, where A_0 is the area of the unstrained surface, then $W_{\text{adh}} \approx (NE_b/A_0)(1 - 2\epsilon)$. This linear relation of W_{adh} on ϵ is plotted as a dashed blue line in Fig. 2. It can be seen that the effect is too small to account for the changes observed in our simulations (solid red line). The difference here indicates that N and/or E_b may change during deformation. Indeed we have found that in some cases more bonds are formed across the interface under compressive strain. This observation can be understood in light of the fact that the strain-induced increase in the density of surface atoms and the change in surface geometry (e.g., a decrease in the interdimer spacing) increase the probability of finding an atom on the countersurface that lies within the interaction range. Calculations of the interfacial energy as a function of strain show that the average energy E_b per bond also increases during compression. Further investigation into the electronic properties of surfaces as a function of strain would be helpful in quantifying the changes in E_b ; however such calculations are not straightforward and are beyond the scope of this paper.

IV. ADHESION OF OXYGEN TERMINATED Si AND SiC

For MEMS/NEMS devices operating in ambient conditions, there will be always oxygen present in the environment. The first step toward a systematic understanding of oxidation effects on adhesion of Si and SiC is to consider surfaces passivated with an increasing amount of oxygen. Early stages of oxidation of Si have been widely studied. For instance, Hoshino *et al.*²⁰ showed that at room temperature and for low oxygen partial pressures ($\sim 10^{-8}$ Torr), native oxide layer on Si surface grows up to 1.5 monolayer (ML) coverage. The subsequent oxide growth is slow and it is limited by diffusion of O through the oxide to the Si/oxide interface. The initial thin oxide layer covers the surface in the form of localized patches rather than as a uniformly distributed layer. As determined by spectroscopy studies reported in Refs. 20 and 21, surface oxide complexes consist of Si^+ , Si^{2+} , Si^{3+} , and Si^{4+} ions, which have been confirmed by *ab initio* calculations of Ciacchi and Payne.²² The most stable oxide complexes have been determined in *ab initio* calculations of Arantes *et al.*²³ It was concluded that there are four basic low-energy positions of oxygen atoms on the Si surface (see Fig. 3): asymmetric and symmetric bridge positions (Br), i.e., when O breaks the Si dimer and bridges the two participating Si atoms, the back bond position (B), i.e., when O attacks the bond between the first and the second layers of Si, and the dangling-bond position (T). Our simulation shows that the symmetric bridge configuration will relax to the asymmetric one and therefore in the discussion

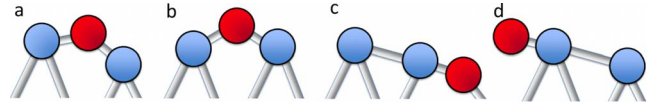


FIG. 3. (Color online) Four basic oxygen configurations on Si surface: (a) asymmetric and (b) symmetric bridge positions (Br), (c) back bond position (B), and (d) dangling-bond position (T). O and Si atoms are dark and light gray, respectively (red and blue).

below Br refers to the asymmetric bridge only. More complicated oxide complexes are formed using the four basic structures as building blocks (e.g., BBr refers to one O atom in the back bond position and another one in the bridge position). In order to establish trends in the adhesion of Si during the early stages of oxidation, we calculate E - d curves for a number of the most stable basic structures.

The early stages of oxidation of SiC are different than those of Si. Our calculations, as well as previous *ab initio* study,²⁴ show that it is not energetically favorable for the O atom to occupy the back bond position between surface Si layer and the underlying C layer. The only energetically stable positions of O on the Si-terminated SiC (001) surface are the symmetric bridge (Br) position analogous to the structure shown in Fig. 3(b). The dangling-bond (T) position, analogous to the one shown in Fig. 3(d), is also possible. However, because the interdimer spacing in SiC is only 3.72 Å, O atom in the T position is able to bridge Si atoms across the interdimer distance, and the T structure relaxes to the symmetric Br position as shown in Fig. 4(a).

We calculated W_{adh} for Si and SiC under different oxygen coverages and the results are shown in Fig. 5. As shown in Fig. 5(a), there is no monotonic trend in W_{adh} of Si with increasing O coverage. However, irrespectively of the specific O configuration, W_{adh} is always positive and the interface is always adhesive. In contrast, W_{adh} of SiC becomes negligible for as little as 1 ML of oxygen coverage [Fig. 5(b)], where no covalent bonds are formed across the interface. It is worth noting that the calculated W_{adh} for oxygen-passivated Si is on the same order of magnitude as the one determined in SFM experiments carried out on Si surfaces coated with native oxide.²⁵

It remains to be explained why oxygen passivation has qualitatively different effects on Si and Si-terminated SiC

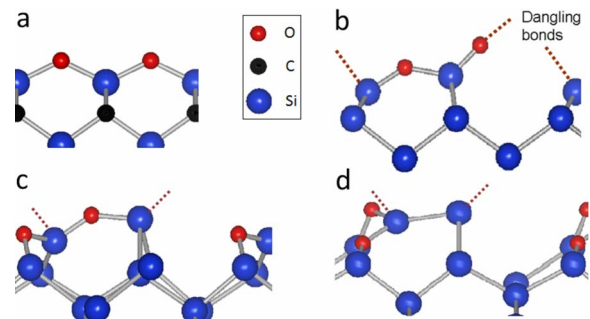


FIG. 4. (Color online) Structures of (a) SiC with 1 ML O, (b) Si with 1 ML O in BrT configuration, (c) Si with 1 ML O in BrB configuration, and (d) Si with 1 ML O in BB configuration. Dashed lines are added to represent the dangling bonds.

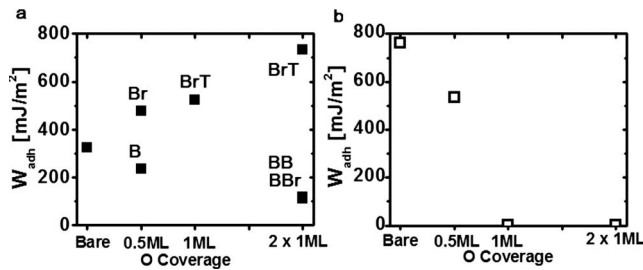


FIG. 5. W_{adh} for surfaces of (a) Si and (b) SiC with varying O coverage. The 0.5 and 1 ML correspond to O passivated surface in contact with a bare countersurface. 2×1 ML corresponds to both surfaces passivated with O. The labels for O complexes on Si are explained in text.

despite strong similarities between the two materials. Understanding of this behavior is brought by structural considerations and has been confirmed by analysis based on the electron localization function. As shown in Figs. 4(b)–4(d), oxygen is not able to bridge the large distance between dimers on Si, leaving dangling bonds on the surface. Such dangling bonds are not present on O-passivated SiC surfaces [Fig. 4(a)] because the smaller interdimer spacing allows O atoms to form bridges between the dimers.

It is the presence of the dangling bonds that makes Si more adhesive than SiC. Specifically, when O-passivated Si surfaces with dangling bonds on O atoms [Fig. 4(b)] are brought together, Si-O-Si bridges begin to form across the interface leading to a significant increase in W_{adh} . If O-passivated Si surfaces have dangling bonds on Si atoms [Figs. 4(c) and 4(d)], covalent bonds will form across the interface between Si atoms. On the other hand, O-passivated SiC surfaces brought together exhibit a large steric repulsion and no covalent bonds are formed across the interface, which is due to the lack of dangling bonds on either Si or O [Fig. 4(a)]. Also it is worth mentioning that in our calculations we only include contributions to the energy that come from direct electronic interactions because standard DFT calculations do not account for long-range dispersive interactions such as van der Waals forces. Including van der Waals interactions would result in an additional weak attraction across the interface for all surfaces considered here. However, because van der Waals forces are orders of magnitude smaller than covalent interactions, we expect that these corrections will have little effect on the trends discovered here. Similar conclusions have been reached by other authors.²⁶

V. CONCLUSION

In conclusion, we determined how adhesion of Si and SiC depends on surface strain and surface chemistry during the early stages of oxidation. Using *ab initio* methods we calculated the energy vs interfacial distance curves for bare surfaces and for surfaces passivated with oxygen. We have shown that Si-terminated (001) SiC surface has larger adhesion than (001) Si surface, which is due to the presence of large compressive surface strain on SiC. We demonstrated that work of adhesion of Si depends linearly on surface strain. Our results also show that while compressive strain leads to increased adhesion on bare surfaces, it aids adhesion reduction as soon as the compressed surfaces are passivated with oxygen.

While the surface strain has been shown to be the dominant phenomenon responsible for the difference between adhesion of SiC and Si, other factors could also affect this difference. For example, SiC is partially ionic (<8%) which is due to the difference in electronegativities of Si and C atoms. Consequently, charge is transferred from Si to C atoms, which is confirmed in our simulations by integrating charges around surface Si atoms on both Si and SiC surfaces. The average charge on Si atoms on SiC surface is 14.6% lower than the average charge on Si atoms on Si surface. Polarization of Si-C bonds can also contribute to adhesion. For instance, polarization has been shown to play an important role in surface reactivity of SiC, i.e., it affects the mechanism of water dissociation.¹³ The effects of charge transfer and polarization on adhesion are currently not well understood.

The discovered dependence of W_{adh} on strain could be used to control adhesion of SiC and Si, which are technologically important materials. The observed interplay between chemistry and strain may offer a possibility of adhesion control not only in MEMS/NEMS design but also in other applications such as wafer bonding.

ACKNOWLEDGMENTS

We gratefully acknowledge financial support from the Air Force Office of Scientific Research (USAFOSR) under Grant No. FA9550-07-1-0126 and from a seed grant in the NSF-funded MRSEC under Grant No. DMR-0520527. Computations were carried out on the NFS Teragrid and on the high performance computer cluster in the Computational Materials Group at UW-Madison.

¹C. Mastrangelo, *Tribol. Lett.* **3**, 223 (1997).

²S. H. Kim, D. B. Asay, and M. T. Dugger, *Nanotoday* **2**, 22 (2007).

³S. T. Patton and J. S. Zabinski, *Tribol. Int.* **35**, 373 (2002).

⁴R. Maboudian and C. Carraro, *Annu. Rev. Phys. Chem.* **55**, 35 (2004).

⁵M. Mehregany and C. A. Zorman, *Thin Solid Films* **355-356**, 518 (1999).

⁶G. Binnig, C. F. Quate, and C. Gerber, *Phys. Rev. Lett.* **56**, 930 (1986).

⁷R. Carpick, D. Ogletree, and M. Salmeron, *J. Colloid Interface Sci.* **211**, 395 (1999).

⁸I. Szlufarska, M. Chandross, and R. W. Carpick, *J. Phys. D* **41**, 123001 (2008).

⁹E. Buks and M. L. Roukes, *Phys. Rev. B* **63**, 033402 (2001).

¹⁰D. Gao, C. Carraro, R. Howe, and R. Maboudian, *Tribol. Lett.*

- 21**, 226 (2006).
- ¹¹Y. Qi and L. G. Hector, *Phys. Rev. B* **69**, 235401 (2004).
- ¹²A. Catellani, G. Galli, and F. Gygi, *Phys. Rev. Lett.* **77**, 5090 (1996).
- ¹³G. Cicero, A. Catellani, and G. Galli, *Phys. Rev. Lett.* **93**, 016102 (2004).
- ¹⁴F. Amy, *J. Phys. D* **40**, 6201 (2007).
- ¹⁵W. R. L. Lambrecht and B. Segall, *Phys. Rev. B* **43**, 7070 (1991).
- ¹⁶M. Kohyama and J. Hoekstra, *Phys. Rev. B* **61**, 2672 (2000).
- ¹⁷G. Kresse and J. Furthmüller, *Phys. Rev. B* **54**, 11169 (1996).
- ¹⁸G. Kresse and J. Furthmüller, *Comput. Mater. Sci.* **6**, 15 (1996).
- ¹⁹J. P. Perdew, S. Kurth, A. Zupan, and P. Blaha, *Phys. Rev. Lett.* **82**, 2544 (1999).
- ²⁰Y. Hoshino, T. Nishimura, T. Nakada, H. Namba, and Y. Kido, *Surf. Sci.* **488**, 249 (2001).
- ²¹H. W. Yeom, H. Hamamatsu, T. Ohta, and R. I. G. Uhrberg, *Phys. Rev. B* **59**, R10413 (1999).
- ²²L. C. Ciacchi and M. C. Payne, *Phys. Rev. Lett.* **95**, 196101 (2005).
- ²³J. T. Arantes, R. H. Miwa, and T. M. Schmidt, *Phys. Rev. B* **70**, 235321 (2004).
- ²⁴E. Wachowicz, R. Rurali, P. Ordejón, and P. Hylgaard, *Comput. Mater. Sci.* **33**, 13 (2005).
- ²⁵A. V. Sumant, D. S. Grierson, J. E. Gerbi, J. A. Carlisle, O. Auciello, and R. W. Carpick, *Phys. Rev. B* **76**, 235429 (2007).
- ²⁶R. Pérez, M. C. Payne, I. Štich, and K. Terakura, *Phys. Rev. Lett.* **78**, 678 (1997).